Vannice, M. A.; Garten, R. L. Influence of the Support on the Catalytic Behaviour of Ruthenium in CO/H_2 Synthesis Reactions. *J. Catal.* **1980**, *63*, 255–260.
Yeh, E. B.; Schwartz, L. H.; Butt, J. B. Silica Supported Iron Nitride in Fischer–Tropsch Reactions. II. Comparison of the Promotion Effects of K and N on Activity and Selectivity. *J. Catal.* **1985**, *91*, 241–253.
Zimmerman, W. H.; Rossin, J. A.; Bukur, D. B. Effect of Particle Size on the Activity of a Fused Iron Fischer–Tropsch Catalyst. *Ind. Eng. Chem. Res.* **1989**, *28*, 406–413.

Received for review September 26, 1989
Revised manuscript received January 29, 1990
Accepted April 9, 1990

Thermal Dehydration of Calcium Hydroxide. 1. Kinetic Model and Parameters

Angel Irabien,* Javier R. Viguri, and Inmaculada Ortiz
Departamento de Ingeniería Química, Facultad de Ciencias, Universidad del País Vasco, Apdo. 644, Bilbao 48080, Spain

In this work, the kinetic model describing the behavior of the dehydration reaction of calcium hydroxide in the range of temperatures 330–450 °C is reported. Two different types of solids have been utilized in dehydration tests: commercial calcium hydroxide, $S = 8.3 \pm 1$ $m^2 \cdot g^{-1}$ and calcium hydroxide reagent obtained in the laboratory under controlled conditions, $S = 18.7 \pm 1.4$ $m^2 \cdot g^{-1}$. A discrimination of the reaction model using the structural parameter ψ of the random pore model led to the best results for a value of $\psi = 0$, which corresponds to a pseudohomogeneous kinetic model of the form

$$\frac{dx}{dt} = k_{S0} \exp(-E_a/RT) \frac{p_0^* \exp(-\Delta H/RT)}{RT} S_0(1 - x)$$

with kinetic parameters $k_s = 1.81 \times 10^{20}$ $cm \cdot s^{-1}$, $E_a = 280.4$ $kJ \cdot mol^{-1}$, $p_0^* = 1.834 \times 10^8$ atm, and $-\Delta H = 138.5$ $kJ \cdot mol^{-1}$. The suitability of the kinetic model to describe the behavior of calcium hydroxide during the dehydration process was confirmed by the results obtained in the correlation of the experimental data of calcium hydroxide reagent, a different solid with a higher surface area.

Introduction

The most commonly used reagents in flue gas desulfurization dry processes are limestone and lime (Ortiz et al., 1987), although recent interest has focused on the hydration of calcium oxide to give calcium hydroxide and the subsequent calcination to produce a highly porous form of CaO (Marsh and Ulrichson, 1985).

Lime sulfation is accompanied by product layer expansion, and thus, the final conversion level is favored by a highly porous structure. The reaction mechanism is not yet fully understood, but several suggestions have been reported (Bhatia and Perlmutter, 1981; Borgwardt and Bruce, 1986; Simons et al., 1987).

The physicochemical properties of the reagent such as specific surface, pore volume, pore size distribution, and particle size distribution are the determining factors in the degree of gas desulfurization as well as in the utilization of the solid sorbent.

Several authors have reported that CaO derived from hydrated lime, $Ca(OH)_2$, is more reactive than that derived from the respective limestone, $CaCO_3$, and even from commercial CaO, yielding higher ultimate conversions of the solid sorbent and thus resulting in greater sulfur capture by $Ca(OH)_2$ (Viguri et al., 1988; Bruce et al., 1989).

Beruto et al. (1980) reported that solid products of decomposing $Ca(OH)_2$ powder at 320 °C under vacuum are particles that have approximately the same exterior dimensions as the parent $Ca(OH)_2$ particles, showing slit-shaped geometry and having higher internal surface areas than does calcium oxide obtained from $CaCO_3$ calcination under vacuum at 510 °C.

Under the conditions usually found in desulfurization processes, the reagent is calcium oxide produced during thermal treatment of calcium hydroxide or calcium carbonate:

$$Ca(OH)_2 \xrightarrow{\Delta} CaO + H_2O \quad (1)$$

$$CaCO_3 \xrightarrow{\Delta} CaO + CO_2 \quad (2)$$

The kinetic behavior of the desulfurization reaction depends on the initial stage of calcium hydroxide dehydration or calcium carbonate calcination. Specially in the case of calcium hydroxide reagent, dehydration takes place at medium temperatures (350–600 °C), depending on the concentration of water vapor in the gas phase, and sintering can interact due to the higher temperature of the desulfurization process (Borgwardt and Bruce, 1986; Mai and Edgar, 1989).

In previous papers, Criado and Morales (1976) studied the mechanism of the thermal decomposition of calcium hydroxide and Mu and Perlmutter (1981) reported the thermal dehydration kinetics of a high-purity calcium hydroxide (98% by weight) under nonisothermal conditions, giving the temperature range of every compound resulting from the decomposition of the initial solid and the reaction kinetics. The results were extremely sensitive to heating rates and decomposition temperatures (325–415 °C), and dehydration kinetics were obtained at the very slow heating rate of 1 °C/min.

The dehydration results were fitted to the linear form of the kinetic equation (Mu and Perlmutter, 1981)

$$dx/dt = k_0 \exp(-E/RT)(1 - x)^{2/3} \quad (3)$$

The estimated parameters were the activation energy, E

* Author to whom correspondence should be addressed.

0888-5885/90/2629-1599$02.50/0

Table I. Chemical Composition of the Commercial Calcium Hydroxide and High Surface Area Calcium Hydroxide

component	av value, %: commer. $Ca(OH)_2$	av value, %: high surface area $Ca(OH)_2$
$Ca(OH)_2$	88.0	78.0
$CaCO_3$	6.0	17.0
CaO	4.2	3.2
SiO_2	0.3	0.3
Al_2O_3	0.1	0.1
Fe_2O_3	0.1	0.1
$CaSO_4$	0.2	0.2
H_2O	0.6	0.6
MgO	0.5	0.5

= 180.0 ± 1.25 kJ·mol^{-1}; the preexponential factor, k_0 = 1.94 × 10^{11} s^{-1}; and the standard error, 4.7%. Criado and Morales (1976) suggested a pseudohomogeneous model:

$$dx/dt = k_0 \exp(-E/RT)(1 - x) \quad (4)$$

The energy of activation was similar to the enthalpy of decomposition, E = 116 kJ·mol^{-1}.

Recently Mai and Edgar (1989) fitted dehydration results using the pseudohomogeneous model, obtaining an activation energy E = 68.3 kJ·mol^{-1} that was assumed to reflect the significance of mass- and heat-transfer limitations in the experimental system.

In this work, the kinetic analysis and modeling of the dehydration reaction of calcium hydroxide are reported due to the interest in the first step of the desulfurization processes using calcium hydroxide as the solid reagent. Two different solid products have been comparatively studied for physicochemical characterization: commercial calcium hydroxide and calcium hydroxide reagent obtained in the laboratory under controlled conditions. A systematic study of the influence on the kinetics of thermoanalytical variables such as sample weight and carrier gas flow rate allows us to separate the coupling between mass transfer and surface reaction kinetics.

Experimental Section

Commercial hydroxide, Dolomitas del Norte S.A., is obtained in the continuous industrial process of lime hydration at high solid/water ratios. Calcium hydroxide is a powderlike solid; therefore, the particle size distribution was determined in a Fritsh Analysette 20 photosettling apparatus, where settling rates were calculated by means of the changes in light absorption by the solid slurry, obtaining a size distribution between 1 and 60 μm. The chemical composition is given in Table I.

Specific surfaces were calculated by application of the standard BET method to nitrogen adsorption isotherms measured in a Carlo Erba Sorptomatic 1800 apparatus. The following results were obtained: commercial calcium oxide, S = 1.1 ± 0.2 m^2/g; commercial calcium hydroxide, S = 8.3 ± 1 m^2/g.

High surface area calcium hydroxide was obtained in a laboratory-scale reactor, in order to know the influence of hydration variables in the final product. Variables were studied in the ranges shown in Table II by means of a factorial design of experiments at two levels. Replicate experiments (five) at the mean values of the hydration variables led to a mean specific surface area of S = 18.7 m^2·g^{-1}, the standard deviation being σ = 1.4 m^2·g^{-1}. It was observed that the linear influence that was evaluated for each variable from the experimental design lied in the experimental error range; therefore, it was concluded that over the range of researched variables they did not present any significant influence on the specific surface area of the

Table II. Experimental Design for the Preparation of Calcium Hydroxide in the Laboratory

variables	level: +	level: −
x_1, particle size, mm	0.40–0.32	0.16–0.08
x_2, liquid-to-solid ratio	100	10
x_3, stirring speed, rpm	600	200
x_4, reaction time, min	60	30
x_5, drying temp, °C	180	110

calcium hydroxide reagent (Viguri, 1989; Viguri et al., 1987).

The pore size distribution was measured in a Micromeritics Poresizer 9310 after mercury penetration. The results show a major contribution of interstices between particles rather than between pores in both solids.

Two different experimental apparatus were utilized to carry out the dehydration experiments: (i) an electric oven, Heraeus M110, provided with a Thermicon P controller allowing for a maximum temperature of 1100 °C; and (ii) a thermobalance, Perkin-Elmer TGA-7, connected to a PE-7500 microprocessor and provided with a TAC-7 controller, GSA-7 gas selector, and GP-2 plotter.

The dehydration experiments under isothermal conditions were performed in the thermogravimetric system using samples between 5 and 25 mg. The reaction atmosphere was controlled through the carrier gas. No difference was found between nitrogen and air as carrier gases, and previous humidification was used in some experiments. Gas flow rates in the range 10–100 mL/min were passed through molecular sieves before entering the thermogravimetric system in the experiments under dry atmosphere.

To reach the temperature of the isothermal experiments, a fast-heating program (≈50 °C/min) was used. Thermogravimetric systems, such as the one described above, allow for the evaluation of the influence of temperature, initial weight of solid, and carrier gas flow rate on the kinetic behavior of the dehydration reaction; however replicate experiments (three) were necessary to obtain experimental errors less than 5% due to the variability of the commercial product.

Kinetic Results and Modeling

The macroscopic description of the experimental system in the thermobalance can be simplified to a piece of metal (D = 0.5 cm, L = 0.3 cm) containing a defined amount (5–25 mg) of small grains of calcium hydroxide, 1 μm ≤ d_p ≤ 60 μm; a carrier gas circulates over the solid, which is heated by an electric furnace. Water vapor produced in the thermal reaction of dehydration diffuses through the product layer in the crucible, which can be considered to be a big particle containing the solid grains, and finally diffuses through the bulk of the carrier gas.

The kinetic behavior of the dehydration reaction of calcium hydroxide can be considered to be the contribution of several resistances corresponding to transfer phenomena and chemical reaction. Four main resistances can be initially established in the experimental system: (i) external mass transfer in the carrier gas, (ii) internal diffusion in the crucible assimilated to a particle containing grains of calcium hydroxide, (iii) internal diffusion through the solid product layer of the grains, and (iv) surface reaction.

Heat transfer would be responsible for the possible temperature gradients in the experimental system.

Dehydration Model. The rate of dehydration of calcium hydroxide depends on the water vapor gradient between the solid interface and the surrounding gas and may be related to the fractional conversion of solid by consid-

ering the change of surface area available for reaction and the diffusion of water vapor. Mathematical relationships have been developed that describe the reaction of a porous solid in terms of the generalized grain model, taking into account the following simplifying assumptions: pseudo-steady-state approximation of the gaseous products within the pellet, solid structure being macroscopically uniform and unaffected by the reaction, isothermal system, diffusion at low concentration of the gas product, and negligible viscous flow contribution to mass transport in the pores.

The approximate solution of the grain model enables us to incorporate the effect of external mass transfer into the solution (Szekely et al., 1976) in general integral form

$$t(p^* - p_e)/RT = \alpha_E(T)x + \beta_p(T)f_P(x) + \gamma_G(T)f_G(x) + \delta_R(T)f_R(x) \quad (5)$$

or in derivative form

$$\frac{dx}{dt} = \frac{(p^* - p_e)/RT}{\alpha_E(T) + \beta_p(T)f'_P(x) + \gamma_G(T)f'_G(x) + \delta_R(T)f'_R(x)} \quad (6)$$

A mass balance for the carrier gas phase, assuming steady-state conditions and taking into account that the evaluation of gas flow rates has been performed at a reference temperature (T_r = 293 K), leads to

$$\frac{dx}{dt} = \frac{p_e/RT}{RT_r n_0/QT} \quad (7)$$

From eqs 6 and 7, the unknown variable p_e can be simplified in the kinetic model, leading to the integral equation

$$t = \{(\alpha_E(T) + RT_r n_0/QT)x + \beta_p(T)f_P(x) + \gamma_G(T)f_G(x) + \delta_R(T)f_R(x)\}RT/p^* \quad (8)$$

According to the grain model, introducing a potential influence of the temperature on mass-transfer parameters $k_g = k_{g0}T^n$ and $D = D_0T^n$, and introducing an exponential influence of the temperature on the reaction parameters $k_s = k_{s0}\exp(-E_a/RT)$,

$$\alpha_E(T) = \frac{V_p(1-\epsilon_p)\rho_s}{A_p k_g} = \frac{n_0}{A_p k_{g0} T^n} \quad (9)$$

$$\beta_P(T) = \left(\frac{V_p}{A_p}\right)^2 \frac{(1-\epsilon_p)\rho_s F_P}{2D_e} = \frac{V_p F_P n_0}{2A_p D_{e0} T^n} \quad (10)$$

$$\gamma_G(T) = \left(\frac{V_g}{A_g}\right)^2 \frac{\rho_s F_g}{2D_g} = \left(\frac{V_g}{A_g}\right)^2 \frac{\rho_s F_g}{2D_{g0}T^n} \quad (11)$$

and

$$\delta_R(T) = \left(\frac{V_g}{A_g}\right)\frac{\rho_s F_g}{k_s} = \left(\frac{V_g}{A_g}\right)\frac{\rho_s F_g}{k_{s0}\exp(-E_a/RT)} \quad (12)$$

By defining a dimensionless temperature $\theta = T/T_0$ and taking the dehydration enthalpy as the parameter describing the influence of the temperature on the water equilibrium pressure, $p^* = p_0^*\exp(-\Delta H/RT) = p_0^*\exp(-h/\theta)$, eq 8 can be transformed into

$$t = (\alpha_0/\theta^m)\exp(h/\theta)x + (\beta_0/\theta^m)\exp(h/\theta)f_p(x) + (\gamma_0/\theta^m)\exp(h/\theta)f_g(x) + \delta_0\theta\exp(g/\theta)f_R(x) \quad (13)$$

Validation of the Kinetic Model. Four independent variables, p_e, n_0, Q, and T, can be used in the experimental system to validate the kinetic model by the conversion–time evolution data; because of the complexity of the model, a sequential analysis of the variables will be performed in order to fit the different hypothesis.

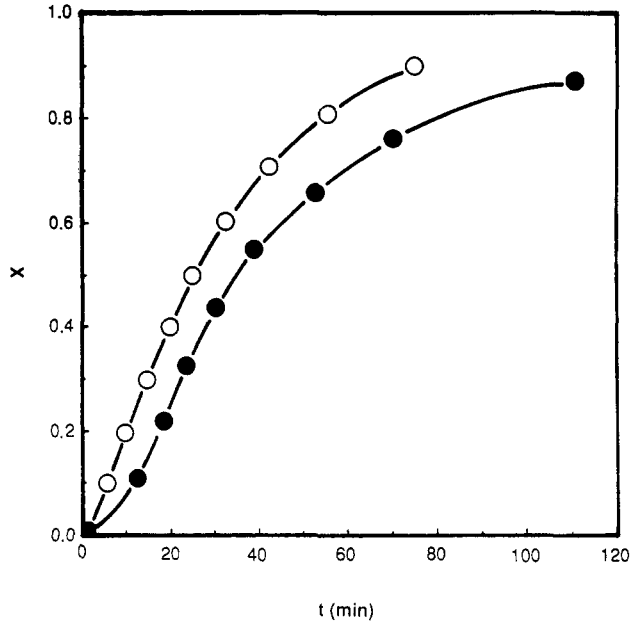

Figure 1. Experimental results of the dehydration in humidified nitrogen. (○) p_w = 0; (●) p_w = 0.0168; T = 673 K; commercial $Ca(OH)_2$.

Influence of the Water Vapor Pressure. During the dehydration of calcium hydroxide, two different phenomena can occur simultaneously depending on the humidity of the gas phase: loss of water from the initial reagent due to the thermal reaction and adsorption of water vapor by the decomposed solid (calcium oxide). The experimental results of the adsorption equilibrium of calcium oxide have been previously reported (Klingspor et al., 1983; Jorgensen et al., 1987).

In order to establish the influence of water vapor pressure on dehydration kinetics, two experiments were performed at 673 K with 22.6-mg calcium hydroxide samples in dry nitrogen and humidified nitrogen, respectively. In the experiments with humidified nitrogen, the gas was passed through an evaporator system with temperature control to set the water concentration in the gas phase. The results are shown in Figure 1. Two main conclusions can be obtained from the experimental curves: (i) adsorption of water on the nascent calcium oxide takes place in the experiment performed at p_w = 0.0168 atm, and (ii) after correction of the experimental curve with maximum conversion, the dehydration rates depend on the water vapor partial pressure.

By using an integral function to relate the time necessary to reach a defined conversion level in dry atmosphere and to that in humidified atmosphere,

$$t_w = F_w(x)(p^* - p_w) \quad (14)$$

$$t = F(x)p^* \quad (15)$$

and assuming the same kinetic behavior in the presence and absence of water vapor, $F(x) = F_w(x)$, from eqs 14 and 15 we thus obtain

$$\frac{t_w}{t} = \frac{p^* - p_w}{p^*} \quad (16)$$

The experimental results of t_w/t are shown in Figure 2 for different conversion levels.

Halstead and Moore (1957) and Matsuda et al. (1985) reported different mathematical expressions for the pre-

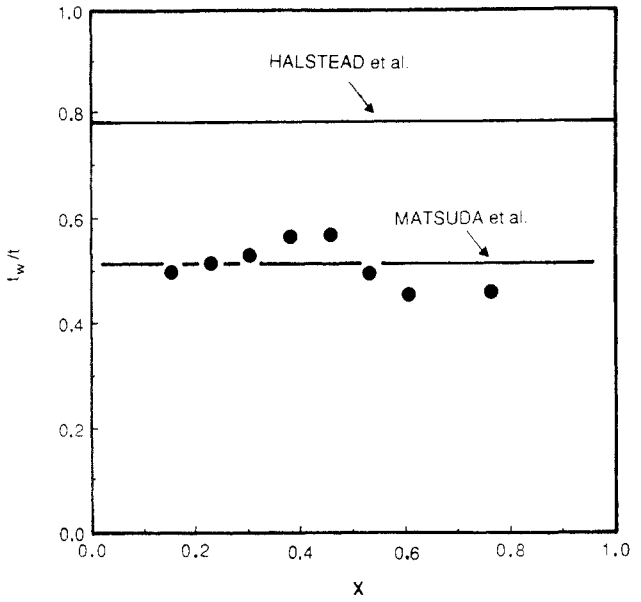

Figure 2. t_w/t at different conversion levels. T = 673 K; commercial $Ca(OH)_2$.

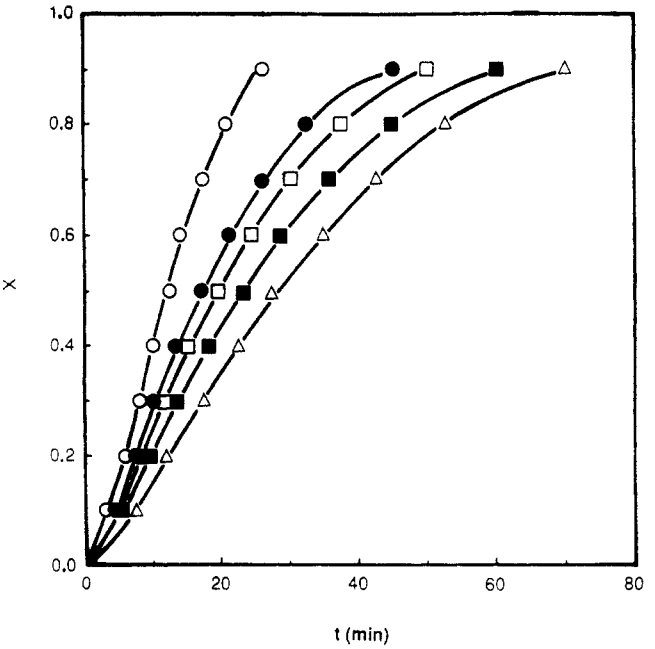

Figure 3. Kinetic experiments with different solid mass. T = 400 °C; Q = 30 $cm^3 \cdot min^{-1}$; (○) w = 5 mg; (●) w = 9.25 mg; (□) w = 13.5 mg; (■) w = 17.75 mg; Δw = 22 mg.

diction of the equilibrium pressure of water vapor as a function of temperature given respectively by

$$p^* = 1.25 \times 10^7 \exp\left(\frac{-12706.4}{T}\right) \quad (17)$$

$$p^* = 1.834 \times 10^8 \exp\left(\frac{-16618.6}{T}\right) \quad (18)$$

The values at 673 K lie on a straight line, Figure 2, checking the validity of the expression of Matsuda et al. (1985) to fit our experimental results.

This fitting indicates that dehydration kinetics are linearly related to the partial pressure gradient of water vapor and equilibrium pressures are fairly well correlated by using eq 18.

Influence of the Initial Mass of the Solid and of the Carrier Gas Flow Rate. Experiments were performed in the thermogravimetric system, where the sample weight and carrier gas (dry nitrogen) flow rate may influence the conversion–time evolution.

The strong influence of the sample weight is shown in Figure 3, for experiments carried out at 673 K.

An evaluation of the external heat- and mass-transfer parameters in the thermogravimetric equipment using water evaporation as a test system leads to the experimental value $k_{g0}A_m = 2.23 \times 10^{-7}$ $cm^3 \cdot s^{-1} \cdot K^{-2.334}$, which can be extrapolated for estimation purposes at 673 K to lead to the values $k_gA_m = 0.889$ $cm^3 \cdot s^{-1}$ and $UA_h = 5.72 \times 10^{-3}$ $cal \cdot s^{-1} \cdot K^{-1}$.

Previous results indicate λ = 138.5 $kJ \cdot mol^{-1}$ and $p^*(673) = 3.46 \times 10^{-2}$ atm, allowing the evaluation of the external temperature gradient and maximum rate of external mass transfer in the experimental system using

$$\Delta T = \frac{N_0\lambda}{UA_h} \quad (19)$$

and

$$\Delta P = N_0/k_gA_m \quad (20)$$

The results of the initial rate of dehydration and estimated temperature gradient are shown in Table III. Temperature gradients less than 1 K do not justify the consideration of external heat transfer in the kinetic analysis.

The maximum rate of external mass transfer at 673 K can be evaluated with eq 20, giving $N_{0max} = 33.49 \times 10^{-6}$ $mol \cdot min^{-1}$, which is very much higher than the experimental values shown in Table III, indicating that $p_e \neq 0$ in the experimental system.

According to eq 13, at constant temperature (673 K), the time necessary to reach a defined conversion as a function of the solid mole number should be given by

$$t = a(\theta,x,Q)n_0 + b(\theta,x) \quad (21)$$

By plotting time values for the same conversion level as

Table III. External Temperature Gradient during $Ca(OH)_2$ Dehydration

10^6N_0, $mol \cdot min^{-1}$	1.955	2.584	3.300	3.862	4.080
ΔT	0.189	0.250	0.320	0.345	0.396

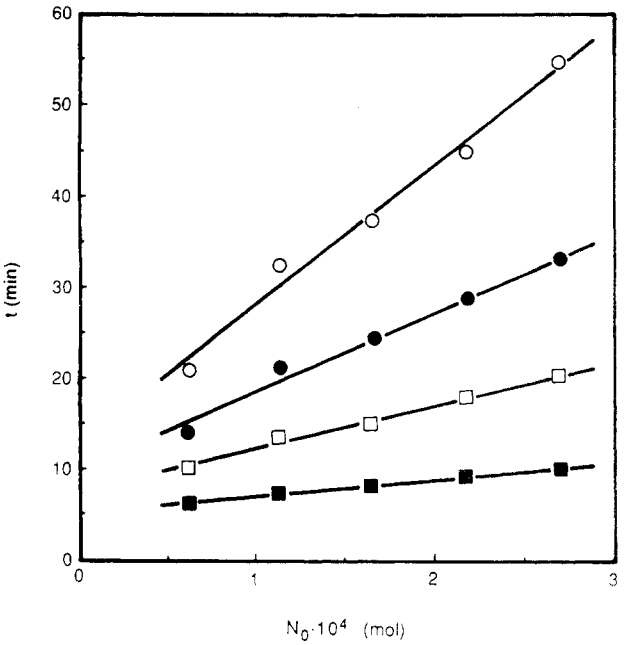

Figure 4. Dehydration time as a function of initial moles of calcium hydroxide. (■) x = 0.2; (□) x = 0.4; (●) x = 0.6; (○) x = 0.8.

Table IV. Parameters of the Linear Regression in Equations 23 and 24

eq	$10^4 a_0$	$10^5 a_1$	r^2
23	6.03	1.57	0.97
24	7.42	1.95	0.99

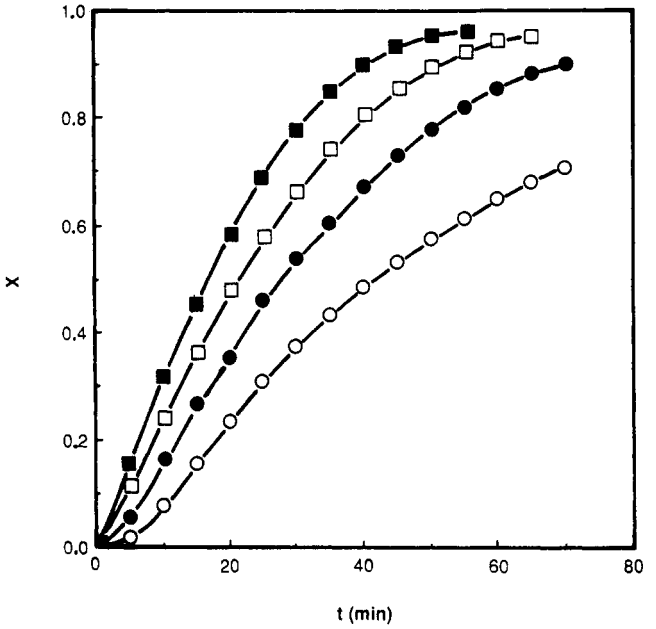

Figure 5. Kinetic experiments at different gas flow rates. T = 400 °C; w = 22 mg; (○) Q = 10 cm^3·min^{-1}; (●) Q = 30 cm^3·min^{-1}; (□) Q = 50 cm^3·min^{-1}; (■) Q = 100 cm^3·min^{-1}.

a function of the calcium hydroxide mole number, Figure 4, a linear relationship can be found between both variables. The origin ordinate encloses the influence of chemical reaction and product layer diffusion, and the slope reflects the influence of the diffusion through the interstices among the grains and the external diffusion.

Taking into account that

$$a/x = a_0(\theta,Q) + a_1(\theta)f_p(x)/x \qquad (22)$$

the slopes of the previous fittings at different conversion can be used to select the particle diffusion model,

plate

$$F_p = 1 \qquad f_p(x) = x^2 \qquad (23)$$

cylinder

$$F_p = 2 \qquad f_p(x) = -(1 - x)\ln(1 - x) \qquad (24)$$

Cylindrical symmetry for the particle shows the best fitting to the experimental results, as is shown in Table IV.

Kinetic experiments for different carrier gas flow rates, w_0 = 22 mg, and T = 673 K are shown in Figure 5. According to eq 13, at constant temperature and solid mole number, the time necessary to reach a defined conversion as a function of the carrier flow rate should be given by

$$t = \frac{c(\theta,x,n_0)}{Q} + d(\theta,x,n_0) \qquad (25)$$

Taking time values at constant conversion, a linear plot of time versus $1/Q$ is shown in Figure 6. Parameters of the linear regression fitting are shown in Table V.

The experimental results indicate that the influence of the external mass transfer and particle diffusion cannot be easily avoided in the experimental system.

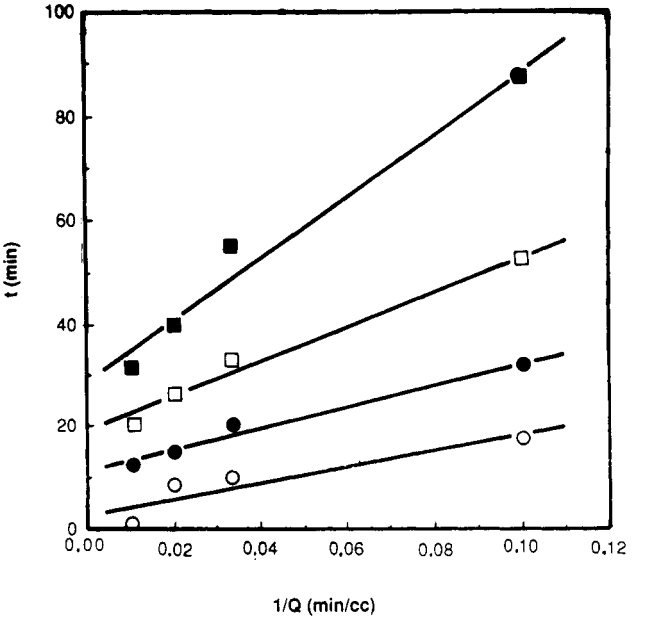

Figure 6. Time values as a function of gas flow rate. (○) x = 0.2; (●) x = 0.4; (□) x = 0.6; (■) x = 0.8.

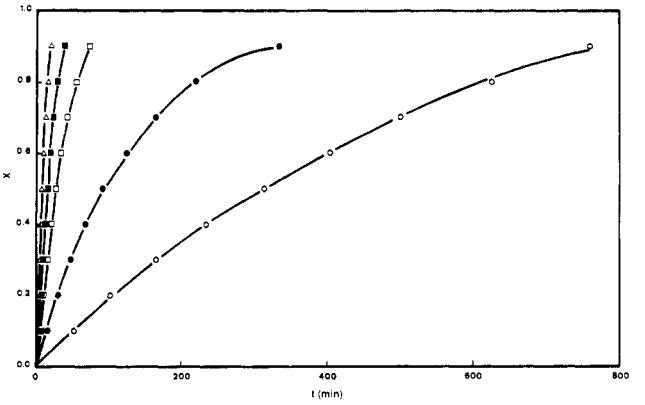

Figure 7. Kinetic results at different temperatures. w = 5 mg; Q = 100 cm^3·min^{-1}; (○) T = 330 °C; (●) T = 342 °C; (□) T = 354 °C; (■) T = 368 °C; (△) T = 380 °C; dry nitrogen.

Table V. Parameters of the Linear Regression Fit to Equation 25

X	d	c	r^2
0.2	156.93	2.05	0.80
0.4	210.62	11.37	0.98
0.6	339.89	19.18	0.99
0.8	600.86	28.84	0.99

Influence of the Temperature. Previous results indicate the strong coupling between transport parameters of the experimental system and dehydration kinetics. The best experimental conditions are related to the minimum sample weight and maximum carrier gas flow rate allowed by the experimental equipment, 5 mg and 100 mL·min^{-1}, respectively.

Isothermal experiments are shown in Figure 7; according to eq 13 at constant conditions of sample weight and carrier gas flow rate, the influence of the temperature should reflect the change in equilibrium pressure (h), diffusion parameters (m), and reaction parameters (g).

A plot of ln t versus $1/T$, Figure 8, indicates the possibility to model the kinetic behavior of the dehydration reaction as a function of the temperature. Examination of Figure 8 leads to the conclusion that two main influences of the temperature should be taken into account. Independent of the conversion level, a dramatic change of the

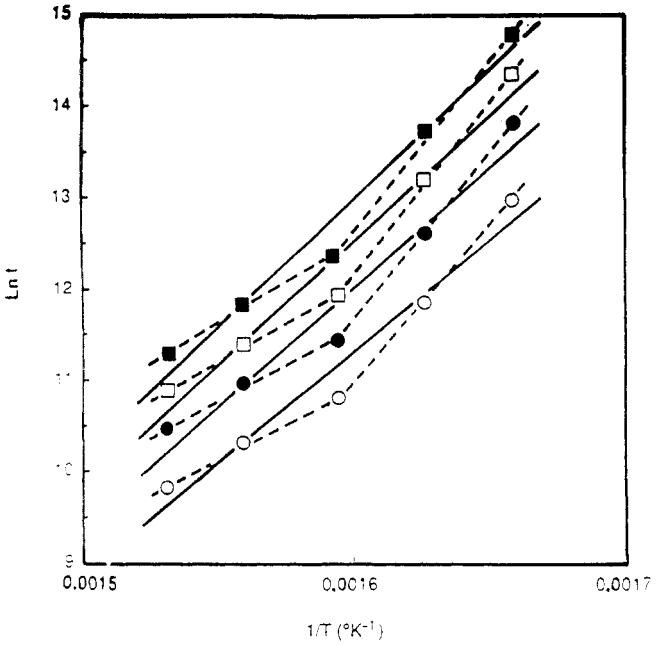

Figure 8. Influence of the experimental temperature on the kinetics of dehydration. n = 2.334; (○) x = 0.2; (●) x = 0.4; (□) x = 0.6; (■) x = 0.8.

slope takes place around 627 K. For temperatures above this value, a slope at around 16 000 K, similar to the dehydration enthalpy ($\Delta H/R$), can be assumed, indicating a mass-transfer control; below 627 K, a much higher slope, approximately 37 500 K (E/R), is necessary to describe the experimental results, indicating a chemical reaction control.

Although experiments have been performed at the most favorable conditions for mass transfer, the results indicate that coupling remains between mass transfer and the chemical reaction.

An evaluation of the experimental results shown in Figure 7 makes the introduction of a defined conversion model necessary for grain diffusion and the chemical reaction. Grain diffusion and reaction in porous grains can be analyzed by using the random pore model (Bhatia and Perlmutter, 1981a,b, 1983), which accounts for the solid structure through a specific parameter, ψ, where

$$f_G(x) = [2/\psi - \ln(1-x)(2/\psi^{1/2})(1/\psi - \ln(1-x))^{1/2}] \quad (26)$$

$$f_R(x) = (1/\psi - \ln(1-x))^{1/2} - 1/\psi^{1/2} \quad (27)$$

A numerical evaluation using a nonlinear regression method based on the Marquardt optimization subroutine of eq 13 in dimensionless form has been performed by using the time necessary to reach a conversion of 0.5 for each experiment, T_0 = 627K, $m = n - 1$ = 1.334, $h = \Delta H/R$, and T_0 = 26.5 and introducing two constant factors of e^{-27} and e^{-80} in the exponential functions to avoid the numerical evaluation of very small numbers for the parameters. Thus, eq 28 has been fitted:

$$\frac{t}{t_{x=0.5}} = \frac{\alpha_0 e^{27}}{t_{x=0.5}\theta^m} e^{26.5/\theta-27} x + \frac{\beta_0 e^{27}}{t_{x=0.5}\theta^m} e^{26.5/\theta-27} f_p(x) + \frac{\gamma_0 e^{27}}{t_{x=0.5}\theta^m} e^{26.5/\theta-27} f_g(x) + \frac{\delta_0 e^{80}\theta}{t_{x=0.5}} e^{g/\theta-80} f_R(x) \quad (28)$$

The best fit has been obtained for the pseudohomogeneous model: $\psi = 0$, $f_R = -[\ln(1-x)]$, cylindrical symmetry for the diffusion in the particle, $f_p = [x + (1-x)\ln(1-x)]$, and negligible influence of the layer product diffusion. The parameter values, the confidence range, and the standard deviation of the parameters are given in Table VI.

Table VI. Best Nonlinear Regression Fit of Equation 28

	$\alpha_0 e^{27}$	$\beta_0 e^{27}$	$\delta_0 e^{80}$	g	σ
parameters	65.83	49.01	11.41	80.17	0.2419
confidence range of the parameters	43.3–88.3	5.9–92	1.23–14.6	68.7–91.6	
std dev of the parameters	11.3	21.5	6.7	5.7	

Discrimination of the best kinetic model has been performed according to non-negative kinetic parameters and previous results of the influence of solid weight and carrier gas flow rate on the kinetic model. Further research on the specific surface evolution during dehydration confirms the linear relationship between the specific surface area and the solid conversion of the pseudohomogeneous model.

Mass Transfer and Reaction Kinetic Constants. From the nonlinear fit to the pseudohomogeneous model, mass-transfer and reaction kinetic constants have been evaluated.

The physical meaning of the fitting parameters are shown in eqs 9, 10, and 12; from α_0, $k_{g0}/(1-\epsilon_p) = 4.325 \times 10^{-6}$ cm·s^{-1}·K$^{-2.334}$. From β_0, $D_{e0}/(1-\epsilon_p) = 1.45 \times 10^{-6}$ cm^2·s^{-1}·K$^{-2.334}$.

Assuming the evaluated external mass-transfer parameter for the experimental equipment, $k_{g0} = 1.137 \times 10^{-6}$ cm·s^{-1}·K$^{-2.334}$ and $1 - \epsilon_p = 0.263$, the effective diffusivity could be $D_{e0} = 3.81 \times 10^{-7}$ cm^2·s^{-1}·K$^{-2.334}$, which agrees well with the diffusion parameter for water in nitrogen (air).

Surface kinetic parameters can be evaluated from δ_0 and g: $k_{s0} = 1.8 \times 10^{20}$ cm·s^{-1}, $E_a/RT_0 = 80.17 - 26.5 = 53.66$, and E_a = 67 296 cal·mol^{-1} = 280.4 kJ·mol^{-1}.

Simulation of the Experimental Results for High Surface Area Calcium Hydroxide. The results of the kinetic experiments performed at 693, 703, and 723 K with a high surface area calcium hydroxide, S_0 = 18.7 m^2·g^{-1}, nitrogen flow rate of 30 mL·min^{-1}, and initial mass of 22 mg allow the validation of the developed kinetic model for different reagents and conditions. The previous correlation can be used taking into account the external mass-transfer parameter,

$$\alpha_R e^{27} = \alpha_0 e^{27}(Q/Q_R)(m/m_R) = 965.51 \text{ min}$$

the particle diffusion parameter,

$$\beta_R e^{27} = \beta_0 e^{27}(m/m_R) = 215.6 \text{ min}$$

and the reaction parameter,

$$\delta_R e^{80} = \delta_0(S/S_R) = 5.19 \text{ min}$$

A simulation can be performed by using eq 29 for the high surface area hydroxide and the experimental conditions previously given:

$$t = \frac{\alpha_R}{\theta^m} e^{26.5/\theta} x + \frac{\beta_R}{\theta^m} e^{26.5/\theta}[x + (1-x)\ln(1-x)] + \delta_R \theta e^{80.17/\theta}[-(\ln(1-x))] \quad (29)$$

The experimental and simulated results are shown in Figure 9, showing the ability of the kinetic model to fit the experimental results of a different calcium hydroxide under different dehydration conditions.

Conclusions

The experimental results of the thermal dehydration of calcium hydroxide indicate the coupling of a high activa-

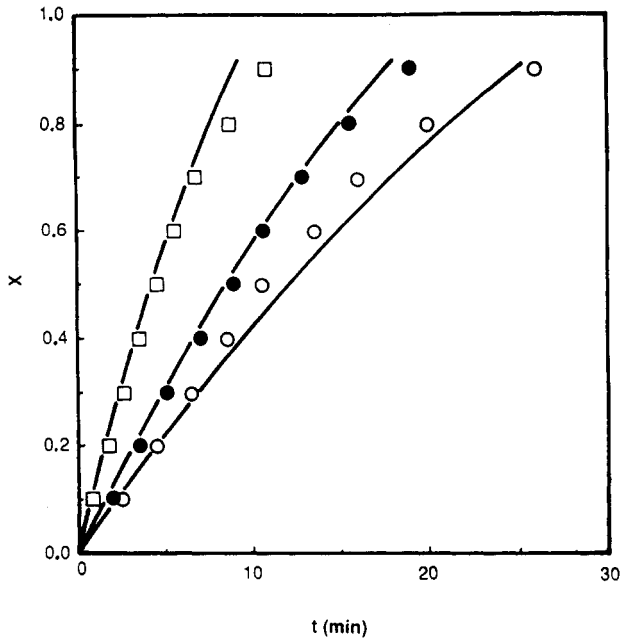

Figure 9. Simulation of dehydration kinetics of calcium hydroxide reagent. (○) T = 420 °C; (●) T = 430 °C; (□) T = 450 °C.

tion energy phenomenon (chemical kinetics) with mass-transfer kinetics.

Nonlinear fitting of the conversion–time curves allows the discrimination between kinetic expressions using the structural parameter ψ of the random pore model as the variable parameter; the best results were obtained for ψ = 0 (pseudohomogeneous model), obtaining the kinetic equation and parameters that allow the simulation of the kinetic behavior of commercial calcium hydroxide and calcium hydroxide reagent obtained under laboratory-controlled conditions.

This work allows the discrimination between mass-transfer kinetics and chemical reaction kinetics in the thermal dehydration of calcium hydroxide. Surface reaction kinetics shows an extremely high value of the activation energy, E = 280.4 kJ·mol^{-1}, leading to a dramatic influence of the temperature on the rate of dehydration and to a strong coupling between surface reaction and mass transfer, which has not been separated in previous works where considerably lower values of the energy of activation have been reported: Criado and Morales (1976), E = 116 kJ·mol^{-1}; Mu and Perlmutter (1981), E = 180 kJ·mol^{-1}; and Mai and Edgar (1989), E = 68.3 kJ·mol^{-1}. The proposed kinetic model and parameters allow the mathematical modeling of the dehydration reaction of calcium hydroxide as the first step of flue gas desulfurization processes using this solid sorbent; the kinetic expression has been seen to be applicable to reagents with different microstructure commercial calcium hydroxide (S = 8.3 m^2·g^{-1}) and calcium hydroxide reagents (S = 18.7 m^2·g^{-1}).

Surface area evolution during the dehydration of calcium hydroxide, which confirms the linear relationship between the specific surface and solid conversion of the pseudo-homogeneous model, will be described in the second part of this work.

Acknowledgment

This work has been financially supported by the spanish CICYT under Project PA86-0147.

Nomenclature

a, b: empirical functions defined in eq 21

a_0, a_1: empirical parameters related to the chemical reaction and product layer diffusion, eq 22

A_g, A_p: external surface area of an individual grain and the pellet, respectively

c, d: empirical functions defined in eq 25

D_e: effective diffusivity of water vapor, cm^2·s^{-1}

D_g: effective diffusivity of water vapor in the product layer, cm^2·s^{-1}

D_0: effective diffusivity independent of the temperature, cm^2·s^{-1}

E: energy of activation, kJ·mol^{-1}

$f_g(x)$, $f_p(x)$, $f_R(x)$: conversion functions referring to the grain diffusion, particle diffusion, and chemical reaction, respectively

F_g, F_p: shape factor for grains and pellets, respectively (=1, 2, nd 3 for infinite slabs, long cylinder, and sphere, respectively)

$F(x)$, $F_w(x)$: conversion functions defined in eqs 14 and 15

g: $(E + \Delta H)/RT_0$

h: $\Delta H/RT_0$

K_gA_m: mass-transfer coefficient, cm·s^{-1}

K_0: preexponential parameter, eq 3, s^{-1}

K_s: kinetic parameter of the surface reaction, cm·s^{-1}

K_{s0}: preexponential parameter of the surface reaction, cm·s^{-1}

m: weight of calcium hydroxide samples, mg

m_R: weight of high surface area calcium hydroxide samples, mg

n: kinetic order of the dependence on temperature of mass-transfer parameters

n_0: initial mole number of the solid compound

N_0: initial mass-transfer rate, mol·min^{-1}

p^*: equilibrium water vapor pressure, atm

p^*_0: equilibrium water vapor pressure independent of the temperature, atm

p_e: external partial pressure of water, atm

p_w: water vapor pressure, atm

Q: gas flow rate in the experiments with commercial calcium hydroxide, cm^3·s^{-1}

Q_R: gas flow rate in the experiments with high surface area calcium hydroxide, cm^3·s^{-1}

S: calcium hydroxide specific surface area, m^2·g^{-1}

S_0: calcium hydroxide specific surface area at t = 0, m^2·g^{-1}

S_R: high surface area calcium hydroxide specific surface area, m^2·g^{-1}

t: time, corresponding to experiments in dry nitrogen

t_w: time, corresponding to experiments in humidified nitrogen

T: temperature

T_0: reference temperature in the kinetic experiments (627 K)

T_r: reference temperature for the gas flow rate (298 K)

UA_h: heat-transfer coefficient, cal·s^{-1}·K^{-1}

V_g: grain volume, cm^3

V_p: particle volume, cm^3

w: solid weight, mg

x: fractional conversion

Greek Letters

α_E, β_P, γ_G, δ_R: kinetic parameters referring to the external diffusion, interparticle diffusion, grain diffusion, and chemical reaction, respectively, eq 5

α_0, β_0, γ_0, δ_0: kinetic parameters independent of the temperature referring to the external diffusion, interparticle diffusion, grain diffusion, and chemical reaction, respectively, eq 28

α_R, β_R, γ_R, δ_R: kinetic parameters referring to the external diffusion, interparticle diffusion, grain diffusion, and chemical reaction, respectively, of the high surface area calcium hydroxide, eq 29

ΔH: dehydration enthalpy, kcal·mol^{-1}

ϵ_p: particle porosity
λ: specific heat of evaporation, kcal·kg^{-1}
ρ_s: molar density of solid
σ: standard deviation
τ: dimensionless time, $t/t_{0.5}$
θ: dimensionless temperature, T/T_0
ψ: structural parameter, defined by Bhatia and Perlmutter (1983)

Registry No. $Ca(OH)_2$, 1305-62-0.

Literature Cited

Beruto, D.; Barco, L.; Searcy, A. W.; Spinolo, G. Characterization of the porous CaO particles formed by decomposition of $CaCO_3$ and $Ca(OH)_2$ in vacuum. *J. Am. Ceram. Soc.* **1980**, *63*, 439-443.

Bhatia, S. K.; Perlmutter, D. D. A random-pore model for fluid-solid reaction II: Diffusion and transport effect. *AIChE J.* **1981a**, *27*, 247-254.

Bhatia, S. K.; Perlmutter, D. D. The Effect of Pore Structure on Fluid-Solid Reactions: Application to the SO_2 lime Reaction. *AIChE J.* **1981b**, *27*, 226-234.

Bhatia, S. K.; Perlmutter, D. D. Unified treatment of structural effects in fluid-solid reactions. *AIChE J.* **1983**, *29*, 281-289.

Borgwardt, R. H.; Bruce, K. R. Effect of Specific Surface Area on the Reactivity of CaO with SO_2. *AIChE J.* **1986**, *32*, 239-246.

Bruce, K. R.; Gullet, B. K.; Beach, L. O. Comparative SO_2 reactivity of CaO Derived from $CaCO_3$ and $Ca(OH)_2$. *AIChE J.* **1989**, *35*, 37-41.

Criado, J. M.; Morales, J. On the thermal decomposition mechanism for the dehydroxylation of alkaline earth hydroxides. *J. Thermal Anal.* **1976**, *10*, 103-110.

Doraiswamy, L. K.; Sharma, M. M. Gas-Solid Noncatalytic Reactions: Analysis and Modeling. Gas-Solid and Solid-Solid Reactions. *Heterogeneous Reactions: Analysis, examples, and reactor design*; John Wiley & Sons, Inc.: New York, 1984; Vol. 1.

Halstead, P. E.; Moore, A. E. The thermal dissociation of calcium hydroxide. *J. Chem. Soc.* **1957**, 3873-3875.

Jorgensen, C.; Chang, C. S.; Brna, T. G. Evaluation of sorbents and additives for dry SO_2 removal. *Environ. Prog.* **1987**, *6*, 26-32.

Klingspor, J.; Karlsson, H. T.; Bjerle, I. A kinetic study of the dry SO_2-limestone reaction at low temperature. *Chem. Eng. Commun.* **1983**, *22*, 81-103.

Lachapelle, D. G. EPA's LIMB technology development program. *Chem. Eng. Prog.* **1985**, *81*, 52.

Mai, M. C.; Edgar, T. F. Surface Area Evolution of Calcium Hydroxide During Calcination and Sintering. *AIChE J.* **1989**, *35*, 30-36.

Matsuda, H.; Ishizu, T.; Lee, S. K. Kinetic study of $Ca(OH)_2$/CaO reversible thermochemical reaction for thermal energy storage by means of chemical reaction. *Kagaku Kogaku Ronbunshu* **1985**, *11*, 542-548.

Marsh, A. W.; Ulrichson, D. L. Rate and diffusional study of the reaction of calcium oxide with sulfur dioxide. *Chem. Eng. Sci.* **1985**, *40*, 423-433.

Mu, J.; Perlmutter, D. D. Thermal decomposition of carbonates, carboxylates, oxalates, acetates, formates and hydroxides. *Thermochim. Acta* **1981**, *49*, 207-218.

Ortiz, M. I.; Viguri, J.; Irabien, A. Generación de energía y contaminación por SO_2. Tecnologías de control. *Energía* **1987**, *2*, 75-88.

Simons, G. A.; Garman, A. R.; Boni, A. A. The kinetics rate of H_2S sorption by CaO. *AIChE J.* **1987**, *33*, 211-217.

Szekely, J.; Evans, J. W.; Sohn, H. Y. Porous solids of unchanging overall sizes. *Gas-Solid Reactions*; Academic Press: New York, 1976.

Viguri, J. R. Hidróxido de calcio como reactivo en desulfuración de gases: Deshidratación y sinterización. Ph.D. Dissertation, The University of País Vasco, Bilbao, Spain, 1989.

Viguri, J.; Ortiz, I.; Irabien, A. Desulfuración de gases. Caracterización de calizas y derivados. *Abstracts of Papers*, 10th Encontro Anual da Sociedade Portuguesa de Química; Sociedade Portugesa de Quimica: Oporto 1987; pp 509-510.

Viguri, J. R.; Diego, L. F.; Ortiz, I.; Irabien, A. Desulfuración de gases. Conversión máxima de compuestos cálcicos. *Abstracts of Papers*, XXII Reunión Bienal de la Real Sociedad Española de Química; R.S.E.Q.: Murcia, 1988; p 382.

Received for review August 25, 1989
Revised manuscript received March 14, 1990
Accepted April 3, 1990

Thermal Dehydration of Calcium Hydroxide. 2. Surface Area Evolution

Angel Irabien,* Javier R. Viguri, Fernando Cortabitarte, and Inmaculada Ortiz
Departamento de Ingeniería Química, Facultad de Ciencias, Universidad del País Vasco, Apdo. 644, Bilbao 48080, Spain

The evolution of the specific surface area associated with the thermal decomposition of calcium hydroxide has been studied experimentally and described by kinetic models utilizing two different solids: commercial calcium hydroxide ($S_0 \approx 8.3$ m^2·g^{-1}) and calcium hydroxide reagent ($S_0 \approx 18.7$ m^2·g^{-1}). The surface area was observed to vary linearly with the fraction decomposed during the dehydration period. Sintering phenomena have been experimentally measured by treating calcium oxide samples ($S_0 \approx 46$ m^2·g^{-1}), obtained after dehydration of calcium hydroxide under constant conditions, at temperatures in the range 500–900 °C for periods of time up to 24 h. A previously developed model, German and Munir (1976), fits the experimental results well if the surface area decreases to less than 55% of the initial value. An empirical kinetic model, where the surface area is linearly related to the heating time, correlates the experimental data, when $\Delta S/S_0 \geq 55\%$. Simulated curves using the obtained kinetic models and parameters, for the specific surface during dehydration and sintering, agree well within the experimental results.

Introduction

Structural changes that take place during the thermal decomposition of calcium hydroxide to give calcium oxide are fundamentally related to the transport processes occurring in some of its reactions with gases that form a solid product. Due to its technological importance, sulfation is the most thoroughly studied reaction of this type.

When calcium hydroxide is thermally treated at intermediate temperatures (350–550 °C), the solid product shows a higher specific surface area than does the initial reagent. Surface generation depends on the kinetics of dehydration; at long times or when decomposition of the initial solid takes place at high temperatures, changes in the surface area and porosity due to sintering phenomena are of considerable importance, decreasing the specific

* Author to whom correspondence should be addressed.

0888-5885/90/2629-1606$02.50/0